

# Numerical simulation of an *in vitro* fibrin clot formation experiment

Eli Bogart

December 12, 2007

## 1 Introduction

The complex process of blood coagulation must lead to the formation of a blood clot which is adequate to stop bleeding while avoiding the formation of a clot which pathologically disrupts circulation. However, the relationship between the dynamics of enzymes involved in coagulation and the morphology of the fibrin network in the resulting clot is not fully understood [1, 2]. Here we present a model of recent coagulation experiments by Wolberg et al [3] which addressed this relationship between dynamics and clot structure and offer some very preliminary results.

## 2 The problem

### 2.1 Biological background

The biochemical processes involved in the initiation of coagulation are highly complex. For the purposes of this project we can drastically restrict our attention to the following portion of the system: initiation of coagulation eventually leads to the formation of prothrombinase, a membrane-bound enzymatic complex which catalyzes the proteolytic conversion of prothrombin, an (inactive) protein present in the plasma, to thrombin. Thrombin then cleaves peptides from fibrinogen, another plasma protein, to form fibrin, which can then polymerize, forming a mesh or clot [4].

### 2.2 Experimental setup

In the experiments of Wolberg et al, layers of cells (fibroblasts or human vascular endothelial cells) were grown in the bottom of wells. When plasma

was added to the wells above the cell layers, coagulation began, and over time a fibrin clot formed. The clot could then be sectioned and the sections imaged to reveal the structure (eg, density) of the clot at various distances from the cell layer.

Variations on the experiment allowed measurement of the total thrombin or fibrin concentration in the well over time after the initiation of coagulation.

Thrombin generation and clot formation were found to be considerably faster over fibroblasts than over HUVEC. The clots had broadly similar structure in that clots over both types of cell were denser near the cell surface, falling to a uniform density from 10-50 micrometers above the surface (and possibly farther.) However, clots over HUVEC consisted of fewer, thicker fibers, while clots over fibroblasts consisted of more numerous thin fibers. This difference in clot quality was attributed to the different levels of thrombin generation, but the details of the relationship between thrombin generation dynamics and clot structure are not clear [3, 5]. The need to explore this interaction further motivates our model of this experimental system.

### 3 Model

We assume that concentrations depend only on vertical position in the well and so model this experiment as a one-dimensional reaction-diffusion problem, tracking the concentrations of prothrombin ( $z$ ), thrombin ( $e$ ), fibrinogen ( $g$ ), fibrin ( $f$ ) and (where we allow a nonzero rate of noncatalytic thrombin-fibrin binding) thrombin bound to fibrin ( $e_f$ ) on the domain  $(0, x_{max})$ , where  $x = 0$  is the cell surface and  $x_{max}$  is the height of the layer of plasma we will simulate (typically less than the actual depth to which the well was filled.) Prothrombin, thrombin and fibrinogen diffuse throughout the domain but fibrin is assumed to be immediately incorporated into a larger polymer upon its production, so fibrin and fibrin-bound thrombin do not diffuse. Thrombin catalyzes the conversion of fibrinogen to fibrin with Michaelis-Menten kinetics and is inactivated (by antithrombin III) with first-order kinetics. When thrombin binds to fibrin noncatalytically, the binding proceeds by mass-action kinetics with one binding site per fibrin monomer (though in fact the availability of binding sites may depend on the polymer structure [6]).

We obtain the following equations governing concentrations in the well:

$$z_t = D_z z_{xx} \quad (1)$$

$$e_t = D_e e_{xx} - k_{one} \cdot (f - e_f) + k_{off} e_f - k_{ine} \quad (2)$$

$$g_t = D_g g_{xx} - \frac{k_{cat} e \cdot g}{k_m + g} - \theta \frac{k_{cat} e_f \cdot g}{k_m + g} \quad (3)$$

$$f_t = \frac{k_{cat} e \cdot g}{k_m + g} + \theta \frac{k_{cat} e_f \cdot g}{k_m + g} \quad (4)$$

$$(e_f)_t = k_{one} \cdot (f - e_f) - k_{off} e_f \quad (5)$$

where  $\theta$  is the ratio of activity of bound thrombin to unbound thrombin. (Using the same  $k_m$  for bound and unbound thrombin is an approximation, as  $k_m$  for bound thrombin, like  $\theta$ , is unknown.)

### 3.1 Boundaries

No-flux boundary conditions are imposed except for thrombin and prothrombin at the cell surface, where we prothrombin is removed and thrombin introduced by a flux given by

$$r = \frac{V_{pro} z(0, t)}{K_{m,pro} + z(0, t)} \quad (6)$$

corresponding to Michaelis-Menten kinetics for activation of prothrombin by a fixed amount of prothrombinase on the cell membranes.

### 3.2 Initial conditions

Following normal values in human plasma, initial concentration of fibrinogen is  $8.2 \mu\text{M}$  [13] and the initial concentration of prothrombin is  $1.4 \mu\text{M}$  [11], both uniform throughout the domain. All other concentration variables are zero initially.

### 3.3 Parameters

Parameter values and their sources are listed in Table 1.

In the absence of a realistic value for the prothrombinase density and corresponding maximum catalytic rate at the cell surface,  $V_{pro}$  was chosen so that (with the indicated  $k_{m,pro}$ ) the maximum rate of thrombin generation in the simulation— the initial rate, before the prothrombin concentration at the cell surface is depleted— equals the maximum observed flux of thrombin into

Parameter	Value	Units	Source
$D_z$	9.5	$\mu\text{m}^2/s$	?
$D_e$	9.5	$\mu\text{m}^2/s$	presumed to equal $D_z$
$D_g$	2	$\mu\text{m}^2/s$	[13]
$k_{cat}$	10	$\text{s}^{-1}$	[10]
$k_m$	12	$\mu\text{M}$	[10]
$k_{in}$	0.02	$\text{s}^{-1}$	[9, 7, 8]
$k_{on}$	0.05	$(\text{s} \cdot \mu\text{M})^{-1}$	completely fictitious
$k_{off}$	0.0005	$\text{s}^{-1}$	completely fictitious
$k_{m,pro}$	0.3	$\mu\text{M}$	[11] citing [12]
$V_{pro}$	10.7	$\mu\text{M}\mu\text{m}/\text{s}$	See text
$\theta$	1 or 0	dimensionless ratio	hypothetical
$x_{max}$	200	$\mu\text{m}$	arbitrary

Table 1: Parameter values and their sources.

the well (8.8  $\mu\text{M}\mu\text{m}/\text{s}$  for fibroblasts, corresponding to a 65.2 nM/minute maximum rate of increase in thrombin concentration in a 225  $\mu\text{L}$  volume over a 0.28  $\text{cm}^2$  base [3, 5].) As the prothrombinase levels in the experiment are not constant, this approximation is of limited accuracy, but should be reasonable if prothrombinase activity rises to near-maximal levels quickly.

The rate of first-order inactivation of thrombin by ATIII was calculated from a rate constant of  $7.7 \pm 0.4 \cdot 10^3$  ( $\text{M} \cdot \text{s}^{-1}$ ) for the *in vitro* association of the substances [9], ATIII's molecular weight (roughly 58000), and a normal plasma ATIII concentration of roughly 150  $\mu\text{g}/\text{mL}$  ([7], citing [8].) The assumption that the concentration of ATIII remains nearly constant for the duration of the experiment or simulation remains to be validated.

For short simulations the choice of  $x_{max}$  is adequate as the concentrations of zymogens  $g$  and  $z$  far away from the cell surface are barely changed; however, on the 30-minute time scale, the supply of fibrinogen is depleted throughout the domain, so a larger spatial domain is called for on that time scale. Results from simulations over long times on a larger spatial domain were not available by press time.

## 4 Implementation

A numerical scheme for this model was implemented in matlab. For each time step the scheme simulates prothrombin diffusion by the Crank-Nicolson method assuming the prothrombin flux set by the surface prothrombin con-

centration at the beginning of the time step remains constant; the results are used to predict the prothrombin concentration at the cell surface at the end of the time step, yielding a corrected flux term. Thrombin and fibrinogen diffusion are then calculated and prothrombin diffusion recalculated (again by Crank-Nicolson), using the corrected flux for thrombin and prothrombin. Finally, the chemical reactions in the bulk medium are updated by fourth-order Runge-Kutta. The code is attached.

The predictor-corrector step for prothrombin addresses problems resulting from the nonlinearity in local prothrombin concentration of the prothrombinase reaction rate; as the reaction pulls prothrombin from the domain, the reaction rate falls more quickly than the local prothrombin concentration, so it is easy to overestimate the net loss of prothrombin over one time step (if, eg, the prothrombin concentration at the beginning of the time step is used to estimate the fluxes at both the beginning and end of the time step), which can lead to oscillatory behavior and in some cases negative thrombin and/or prothrombin concentrations near the boundary. Even with this predictor-corrector method these problems can still appear when a long time step (above about 10 ms, with the current parameter values) is employed.

The simulations presented here used a time step  $k = 0.005$  s and a spatial grid spacing of 10 nm in the first micrometer above the cell surface, 50 nm from 1 to 10  $\mu\text{m}$  above, 100 nm from 10 to 30  $\mu\text{m}$  above, 200 nm from 30 to 50  $\mu\text{m}$  above, and 500 nm from 50 above out to  $x_{max}$ .

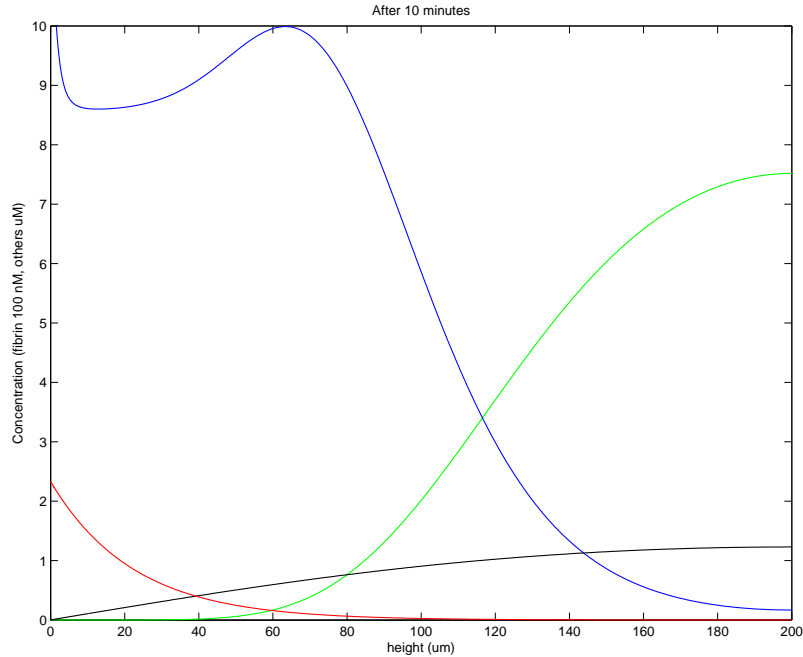
## 5 Results

To test the model and explore the issue of noncatalytic thrombin-fibrin binding, simulations with and without thrombin-fibrin binding and with either zero activity of bound thrombin or a bound thrombin activity equal to that of free thrombin.

### 5.1 No thrombin-fibrin binding

Fig. 1 shows the results without thrombin-fibrin binding. A substantial clot appears to have formed out to about 100 microns from the cell surface. The steep fall in fibrin concentration in the first 10 microns followed by a relatively uniform concentration for some distance qualitatively agrees with experimental results but the rise in concentration starting around 40 microns from the base was not observed in experiments. Zymogen concentrations in

Figure 1: Simulated concentrations of fibrin (blue), fibrinogen (green), thrombin (red) and prothrombin (black) vs height above the layer of cells at the base of the well, 10 minutes after initiation of coagulation. No thrombin-fibrin binding allowed.



the far field are not substantially depleted after 10 minutes validating this choice  $x_{max}$ .

## 5.2 Thrombin-fibrin binding but bound thrombin inactive

Fig. 2 shows the results when we allow noncatalytic thrombin-fibrin binding. The resulting clot is found almost entirely within 40 microns of the cell surface (and within 20 microns of the surface is much more dense than any part (except very close to the cells) of the clot we found above without thrombin-fibrin binding. This indicates, and observed distributions of bound and free fibrin confirm, that binding to the growing fibrin clot substantially hinders the diffusion of thrombin. Noting that the bound thrombin plot has different units than the free thrombin plot, we see that much more bound thrombin than free thrombin is present, reflecting the assumption (not nec-

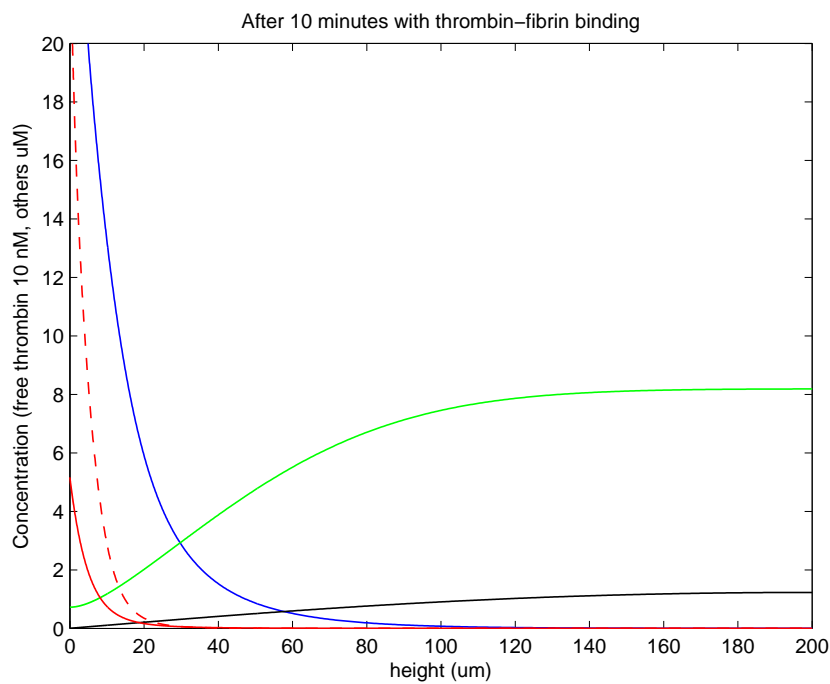


Figure 2: Simulated concentrations of fibrin (blue), fibrinogen (green), free thrombin (red), thrombin bound to fibrin (dashed red line), and prothrombin (black) vs height above the layer of cells at the base of the well, 10 minutes after initiation of coagulation. Thrombin bound to fibrin is inactive.

essarily valid!) that bound thrombin is protected from ATIII inhibition.

### 5.3 Thrombin-fibrin binding, bound thrombin active

When the bound thrombin is allowed to retain its fibrinogenic activity the resulting distribution of fibrin (shown in Fig. 3) is a narrow peak at about 25 microns from the cells (with a very thin layer of higher concentration next to the cell surface.) It is not immediately clear how this is achieved. Note that such steep variations in fibrin concentration would in reality probably be blurred by the diffusion of fibrin monomers before the bind to the mesh.

## 6 Conclusion

The results suggest fibrin-thrombin binding could have substantial impact on clot structure. Further, the results are promising in that they demonstrate the potential of the model, as implemented, to produce vaguely plausible results and interesting if inexact predictions. Recent improvements in the speed of the simulation should allow for exploration of more of the parameter space, and the model can easily be extended to incorporate a basic representation of the structure of the fibrin clot (tracking concentrations of monomers, thin fibers, and thick fibers, eg.) which is one immediate goal of future work.

However, the primary obstacle to serious attempts to reproduce the experimental results or to produce realistic results from hypothetical cases, remains the difficulty of accurately capturing the activity of the membrane-bound prothrombinase, for which better parameters and possibly a different modelling approach are necessary. Without more confidence in this aspect of the the model it will be difficult to address the major issue raised by the current experimental results– the differences between clots formed over fibroblasts and vascular endothelial cells, which (presumably) originate in levels of prothrombinase activity which evolve differently over time. A different numerical approach to thrombin is also indicated as the problem of oscillatory prothrombin concentrations near the boundary is currently what limits the choice of time step. Refining the approach to prothrombinase is consequently the most urgent next step in developing the model.

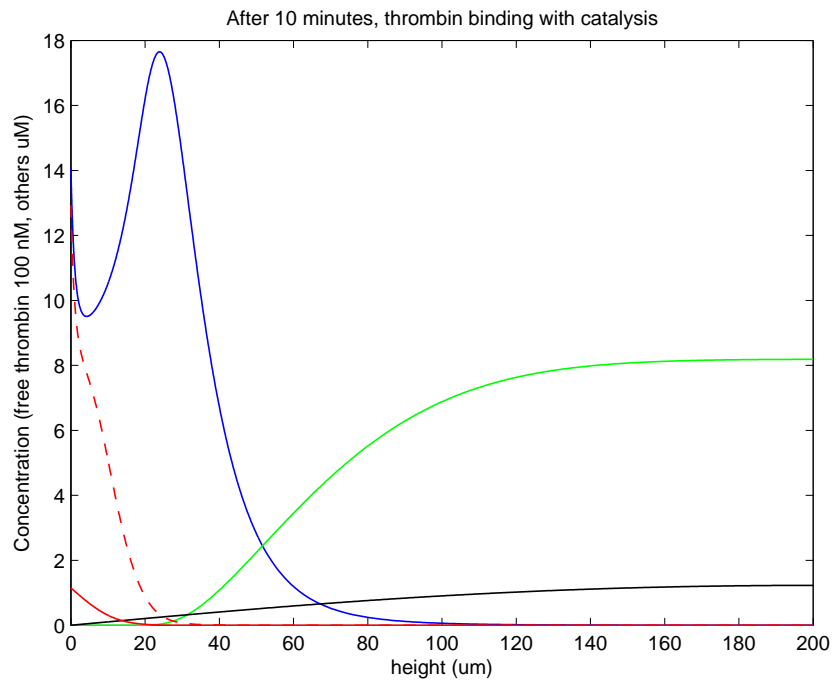


Figure 3: Simulated concentrations of fibrin (blue), fibrinogen (green), free thrombin (red), thrombin bound to fibrin (dashed red line), and prothrombin (black) vs height above the layer of cells at the base of the well, 10 minutes after initiation of coagulation. Thrombin bound to fibrin is as active as free thrombin.

## References

- [1] A.S. Wolberg, "Thrombin generation and fibrin clot structure", *Blood Reviews* 21:131-142 (2007).
- [2] D.M Monroe and M. Hoffman, "What Does It Take to Make the Perfect Clot?", *Arterioscler Thromb Vasc Biol* 26:41-48 (2006).
- [3] R.A. Campbell, K.A. Overmyer, C.R. Bagnell, and A.S. Wolberg, "Differing Procoagulant Activities of Different Cell Types and Their Role in Fibrin Clot Formation". Poster.
- [4] J. Jesty and Y. Nemerson, "The pathways of blood coagulation", in *Williams Hematology*, 5th ed, E. Beutler et al, Eds. New York: McGraw-Hill, 1995, pp. 1227-1238.
- [5] A.S. Wolberg, personal communication, October 2007.
- [6] H. Bänniger, B. Lämmle, and M. Furlan, "Binding of  $\alpha$ -thrombin to fibrin depends on the quality of the fibrin network", *Biochem J* 298:157-163 (1994).
- [7] R.D. Rosenberg, "The Heparin-Antithrombin System: A Natural Anticoagulant Mechanism", in *Hemostasis and Thrombosis: Basic Principles and Clinical Practice*, 2nd ed., R.W Colman, J. Hirsh, V.J Marder, and E.W. Salzman, Eds. Philadelphia: J.B. Lippincott, 1987.
- [8] G. Murano, L. Williams, M. Miller-Anderson et al, "Some properties of antithrombin III and its concentration in human plasma", *Thromb Res* 18:259 (1980).
- [9] S.T. Olson, R. Swanson, E. Raub-Segall, T. Bedsted et al, "Accelerating ability of synthetic oligosaccharides on antithrombin inhibition of proteinases of the clotting and fibrinolytic systems: comparison with heparin and low-molecular-weight heparin", *Thromb Haemost* 92:929-939 (2004).
- [10] R.R. Hantgan and J. Hermans, "Assembly of Fibrin: A Light Scattering Study", *J Biol Chem* 254:11272-11281 (1979).
- [11] A.L. Kuharsky and A.L. Fogelson, "Surface-Mediated Control of Blood Coagulation: The Role of Binding Site Densities and Platelet Deposition", *Biophys J* 80:1050-1074 (2001).

- [12] M.E. Nesheim, R.P. Tracy, P.B. Tracy, D.S. Boskovic, and K.G. Mann, "Mathematical simulation of prothrombinase", *Methods Enzymol* 215:316-328 (1992).
- [13] J.W. Weisel, "Fibrinogen and Fibrin", *Advances in Protein Chemistry* 70:247-299 (2005).